

Hydroxyl concentration estimates in the sunlit snowpack at Summit, Greenland

Andreas J. Beyersdorf^{a,*}, Nicola J. Blake^a, Aaron L. Swanson^b,
Simone Meinardi^a, Jack E. Dibb^c, Steve Sjostedt^d, Greg Huey^d, Barry Lefer^e,
F. Sherwood Rowland^a, Donald R. Blake^a

^aDepartment of Chemistry, University of California at Irvine, Irvine, CA 92697-2025, USA

^bAtmospheric Chemistry Division, NCAR, Boulder, CO 80305, USA

^cInstitute for the Study of Earth, Oceans, and Space, University of New Hampshire, Durham, NH 03824-3525, USA

^dSchool of Earth and Atmospheric Sciences, Georgia Institute of Technology, Atlanta, GA 30332-0340, USA

^eGeosciences Department, University of Houston, Houston, TX 77204-5007, USA

Received 1 August 2005; accepted 10 August 2006

Abstract

Experiments were performed at Summit, Greenland (72°34' N, 38°29' W) to investigate hydroxyl mixing ratios in the sunlit surface snowpack (or firn). We added a carefully selected mixture of hydrocarbon gases (with a wide range of hydroxyl reactivities) to a UV and visible light transparent flow chamber containing undisturbed natural firn. The relative decrease in mixing ratios of these gases allowed estimation of the lower limit mixing ratio of hydroxyl radicals in the near-surface firn pore spaces. Hydroxyl mixing ratios in the firn air followed a diurnal cycle in summer 2003 (10–12 July), with peak values of more than 3.2×10^6 molecules cm^{-3} between 13:00 and 16:00 local time. The minimum value estimated was 1.1×10^6 molecules cm^{-3} at 20:00 local time. Results during spring of 2004 showed lower, but rapidly increasing, peak hydroxyl mixing ratios of 1.1×10^6 molecules cm^{-3} in the early afternoon on 15 April and 1.5×10^6 molecules cm^{-3} on 1 May. Our firn hydroxyl estimates were similar to directly measured above-snow ambient levels during the spring field season, but were only about 30% of ambient levels during summer.

© 2007 Elsevier Ltd. All rights reserved.

Keywords: Snowpack photochemistry; Firn air; Hydroxyl; Summit

1. Introduction

Hydroxyl radical (OH) is the primary oxidant in the earth's atmosphere. High humidity and small solar zenith angles contribute to large OH levels in the tropical marine boundary layer. Conversely,

hydroxyl concentrations in Polar Regions have traditionally been expected to be much lower. However, Mauldin et al. (2004) reported typical OH concentrations of $(2.5\text{--}3.5) \times 10^6$ molecules cm^{-3} above the snow at South Pole. In addition, at Summit, Greenland (72°34' N, 38°29' W, 3200 m elevation), the model of Yang et al. (2002) predicted OH levels of more than 4×10^6 molecules cm^{-3} . This level is 3 times that expected based on ozone

*Corresponding author. Tel.: +1 949 824 5457;
fax: +1 949 824 2905.

E-mail address: abeyersd@uci.edu (A.J. Beyersdorf).

photolysis alone. These results are based on elevated concentrations of OH precursors such as nitrous acid (HONO), formaldehyde (HCHO), and hydrogen peroxide (H_2O_2) measured in the summer boundary layer. Recent research has shown that HONO (Zhou et al., 2001), HCHO (Hutterli et al., 1999; Sumner and Shepson, 1999; Jacobi et al., 2002), and H_2O_2 (Hutterli et al., 2001) are produced in the snowpack and released to the atmosphere.

Direct ambient OH measurements made at Summit during the summer of 2003 peaked at 25×10^6 molecules cm^{-3} (Sjostedt et al., 2007). However, OH concentrations in the firn air (air which fills the pore spaces of the snowpack) may differ. Heterogeneous processes that are not feasible in the gas phase can take place on the liquid phase of snow grains. The photolysis of OH precursors such as HONO and H_2O_2 in the liquid phase can act as a source of OH that may be transported to the firn air and boundary layer. Also, partitioning between the firn air and snow grains may be an additional loss for OH in the firn air. If the OH is partitioned into the quasi-liquid layer present on the snowgrains it is not likely to desorb. So, to better understand the chemistry of the OH at Summit it is necessary to determine what its concentration is in the snowpack.

Unfortunately, the high reactivity of hydroxyl makes direct measurement of its concentration in the snowpack impossible using existing techniques. Attempts to draw air from the snow to the instrument would result in complete loss of hydroxyl on the tubing walls. This problem prompted us to develop an indirect OH approximation method involving the addition of a gaseous mixture of compounds into the firn. The relative decay of these gases in relation to their hydroxyl reactivity was then used to approximate the hydroxyl concentration.

A similar method had been employed in several previous field seasons at Summit, Greenland (Blake et al., 1999; Swanson et al., 2000) to attempt to quantify snowpack OH radical concentrations. However, these attempts were not successful for several reasons. First, the hydrocarbon mixture employed contained only unbranched alkanes, which along with having a wide range of hydroxyl reactivities, also have a wide range of diffusion coefficients. This resulted in apparent decay rates for the suite of alkanes that were in fact more a function of their relative diffusion rates through the snow pore spaces (analogous with chromatographic

separation), rather than their differential removal by OH. For the field campaigns of 2003 and 2004, this problem was resolved by employing only a suite of butenes, which have similar diffusion coefficients but varying reactivity with OH.

Attempts previous to 2003 also did not fully characterize the background concentrations of the nonmethane hydrocarbons (NMHCs) in the snow before any of the hydrocarbon mixture was added. During 2003 and 2004, numerous samples were collected inside the chamber before the experiments were performed. Finally, we have learned that a consistent air flow rate through the chamber is essential for proper OH estimation. The flow was regulated for the experiments reported here.

2. Methods

The method we employ for indirect estimation of near-surface snow pore air OH radical mixing ratios consisted of adding reactive NMHCs through a probe into the snow and withdrawing air through two other probes to monitor hydrocarbon decay over time. By looking at the relative decay of these compounds in relation to their rate of reaction with OH, we estimated the average hydroxyl concentration. A disadvantage of this method is the fact that the addition of species with high OH reactivities will lower the concentration of hydroxyl in the snow. Therefore the OH mixing ratios calculated here define lower limit values. Unfortunately, this underestimation cannot be quantified without better knowledge of the production rate of hydroxyl. The sources of hydroxyl in the firn air still are not fully known. As such it is not possible to determine the rate at which the hydroxyl is replenished in the firn air.

3. Experimental techniques

These experiments were performed as part of a larger study of the hydroxyl budget associated with sunlit snow. This project included measurements of chemical species and actinic flux in and above the snowpack. The first field season measurements were made in June and July, 2003. During this time period, the arctic region has 24 h of sunlight and photochemistry should be at its maximum. A second field season occurred from March to early May, 2004. During this period, Summit experiences rapidly increasing day lengths, from approximately 12 h of sunlight in mid-March to 22 h of direct sunlight in early May.

Our experiments were performed at a satellite science camp 1 km south of the power generators and living quarters of the main Summit camp. The predominant wind direction is from the south; therefore pollution plumes from the camp generators rarely reached the site.

A reaction chamber was set up in an undisturbed section of snow. The rectangular chamber was made of Acrylite OP4 plastic. This plastic is transparent to UV and visible light with transmittance of over 80% at wavelengths above 300 nm. Two parallel vertical panels were carefully inserted into the snowpack. Another panel was placed between these side panels on top of the snow (Fig. 1). The placement of this top panel was done in a manner in which to minimize the headspace above the snow. However it was impossible to ensure perfect contact with the surface snow. At one end a baffle (also made of Acrylite OP4 plastic) was connected to the three panels. All panels and the baffle were “glued” together by freezing ultrapure water in the seams. Excess water was used in order to minimize leakage through the seams. Although desirable, placement of a bottom panel to the chamber was deemed impossible without an unacceptable amount of disturbance of the natural snow. Therefore, the opposite end and the bottom of the chamber were left open. A bellows pump was connected to the baffle, pulling air (ideally) through the entire cross section of the firn inside the chamber. The flow rate of air pumped through the chamber was stabilized by the use of a regulator connected to the pump inlet. The flow rate was measured multiple times during the experiment to check the consistency of the regulator.

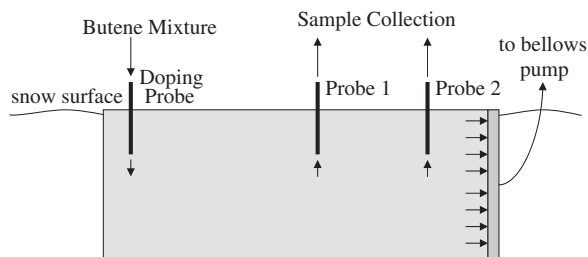


Fig. 1. Schematic of the snow chamber setup. The chamber was 110 cm in length with a width and depth in the snow of 40 cm. Probes were made of stainless-steel tubing and placed with their ends 5 cm into the snow. The distance between the doping probe and probe 1 was 64 cm in 2003 and 32 cm in 2004. The distance between probes 1 and 2 was 32 cm. Arrows show the flow of air through the chamber.

The rectangular chamber had dimensions of 110 cm long and 40 cm wide with an open bottom and end. The side panels extended 40 cm into the snow. The top panel on the chamber had three holes in it that were each large enough for the insertion of a stainless-steel probe. Each probe was sealed in place by freezing enough water around them that we could assume there to be no leakage. The first probe (labeled “doping probe” in Fig. 1), was used to continuously dope in the hydrocarbon mixture. After allowing the system to equilibrate, simultaneous samples were withdrawn through the other two probes. In 2003, probes 1 and 2 were at a distance of 64 and 96 cm, respectively, from the doping probe. In 2004, these holes were located 32 and 64 cm from the doping probe. The probe tubes extended to a depth of 5 cm into the snow and were connected via stainless-steel tubing to separate bellows pumps throttled to draw air from the chamber at a continuous flow rate of about 0.5 L min^{-1} . Our 2 L stainless-steel canisters (housed along with the pumps in a ski-equipped temperature-controlled lab) were pressurized to at least 20 psig.

The gaseous hydrocarbon mixture added into the snow-filled chamber consisted of nine C_2 – C_7 alkanes, nine C_4 – C_6 alkenes, four C_2 – C_4 alkynes, two CFCs, two HCFCs, and one halon. This mix was used in order to have a wide range of reactivities with OH. However, for the hydroxyl calculations only the butenes (1-butene, *iso*-butene, *cis*-2-butene, and *trans*-2-butene) were used due to their similar diffusion coefficients. The mixture was continuously doped into the chamber at a constant flow rate of 1 – 2 L min^{-1} during each experiment. Samples were not collected until at least 2 h after the start of the doping. This allowed for the mixture to flow through the chamber and reach a pseudo-steady state gradient throughout the snow.

The experiments were performed during periods of light wind to reduce variation in air flow. Tests employing the addition of a discrete spike of sulfur hexafluoride (SF_6) were performed to determine optimum pumping rates for the three pumps and to estimate the residence time of the air flow between the two probes, τ . We believe that the difference between diffusion coefficients of SF_6 and the butenes should have little effect on the residence time (but will cause a significant difference in the relative loss of SF_6 seen at the second probe). A 5 ppmv sample of SF_6 was injected into the chamber through a septum attached to the doping probe.

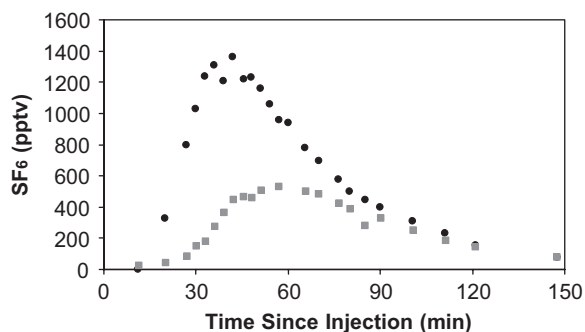


Fig. 2. Results of an SF₆ test performed on 9 July, 2003. Circles represent the SF₆ concentration in samples collected from probe 1. Squares represent probe 2 samples.

Samples were then collected by syringe through septums attached to the other probes. The SF₆ samples were analyzed with an on-site gas chromatograph (GC, a Lagus Applied Technology Automatic Tracer Gas Monitor with an electron capture detector (ECD), limit of detection for SF₆ of 50 pptv). Fig. 2 illustrates the results of one of these tests, performed on 9, July 2003. The SF₆ curves for each probe were integrated to find the area. Finding the time at which half of this area is under the curve approximates the time at which 50% of the sample had arrived at each probe. The Δ time for the two sampling probes was determined for the times corresponding to 30%, 40%, 50%, 60%, and 70% of the sample area. The average of these times was then used to estimate the residence time, τ , while the standard deviation represented the error in τ . For example, for the 9 July test (Fig. 2) τ was determined to be 16.9 ± 1.6 min. The broadness of the peaks seen in Fig. 2 is mainly due to diffusion of the gases through the chamber. The absence of a bottom panel is also likely to have caused some of the flow variability. However, the presence of stratified layers in the snow and the constant horizontal flow likely reduced the importance of vertical diffusion.

4. Trace gas analysis

Upon completion of the field experiment, the sampling canisters were returned to the laboratory at the University of California, Irvine for analysis. NMHCs, halocarbons, and alkyl nitrates were measured via a 3 GC system, described in Colman et al. (2001). In 2003, the system employed a quadrupole mass selective detector (MSD), 2 flame ionization detectors (FIDs), and 2 ECDs. The

samples in 2004 were analyzed on the same system with the exception that a sixth column-detector channel consisting of a cyclodex column output to a FID was added.

In brief, an aliquot of each sample is pre-concentrated in a stainless-steel loop containing glass beads cooled with liquid nitrogen. Heating the loop re-volatilizes the sample. The sample is then flushed by a helium carrier and split into six streams each output to a different column-detector combination. The ECDs are used to quantify halocarbons and alkyl nitrates, the FIDs are sensitive to hydrocarbons, and the MSD is set for selective ion detection. Butenes were quantified through the use of two of these column-detector channels. The first used a 60 m J&W DB-1 column outputted to an FID. The second was a 30 m PLOT column connected to 5 m of a DB-1 column with output to another FID. The detection limit for each butene is 3 pptv. The precision of our butene analysis was tested during the Nonmethane Hydrocarbon Inter-comparison Experiment (NOMHICE) and was found to be $\pm 2\%$ (Sive, 1998).

5. Hydroxyl estimation

Seasonal NMHC data collected at Summit indicate that the dominant removal process of these NMHCs is reaction with the OH (Swanson et al., 2003). If we assume that OH is the only oxidant, the kinetic rate law of a compound (A) can be written as

$$d[A]/dt = -k_{OH}[OH][A]. \quad (1)$$

Integrating this equation leads to

$$\ln[A] = -k_{OH}[OH]t + \text{constant}. \quad (2)$$

If the concentrations of A sampled at probe 1 and 2 are, respectively, labeled as $[A]_1$ and $[A]_2$, this gives

$$\ln([A]_2/[A]_1) = -k_{OH}[OH]\tau, \quad (3)$$

where τ is the residence time for compound A to go from probe 1 to probe 2. The more negative this natural log value is, the more decay has occurred.

Eq. (3) assumes that the only mechanism of loss is chemical reaction with OH. Therefore, the presence of secondary oxidants could increase apparent OH mixing ratios. Halogen chemistry is unlikely to play a large role due to the remote distance of Summit from the coast, but its role is being investigated (Peterson and Honrath, 2001; Sjostedt et al., 2007). Ozone, present in the firn at concentrations of between 20 and 40 ppbv, reacts with butenes at a

much slower rate than OH. The lifetime of butenes due to ozone alone is therefore 2 orders of magnitude longer than their respective hydroxyl lifetimes, making it unlikely that reaction with ozone represents a significant sink. As mentioned above, a potentially important effect that would reduce apparent OH levels is the competition for OH represented by the reactive hydrocarbons in the mix with the butenes.

Diffusion also plays a large role in increasing the apparent decay of the compound as it moves through the snow. By selecting compounds with comparable diffusion coefficients, we have ensured that the relative decrease in concentration due to the reaction term will dominate. Therefore, if the $\ln([A]_2/[A]_1)$ values for a group of compounds with the same diffusion coefficient are graphed versus their k_{OH} s the slope will be equal to

$$\text{Slope} = -[\text{OH}]\tau, \quad (4)$$

with τ determined from the SF₆ tests described here.

The group of gases used to determine the hydroxyl concentration was the butenes (1-butene, *iso*-butene, *cis*-2-butene, and *trans*-2-butene). Their temperature-dependant rate constants with OH are well studied and our GC analysis for these gases has high accuracy and precision. These molecules also exhibit good stability in our pressurized sampling canisters at the mixing ratios employed in this experiment. A drawback to this method is the production of small amounts of 1-butene and *iso*-butene in sunlit natural snow (Swanson et al., 2002).

Background samples (firn air sampled from the chamber when the hydrocarbon mix was not being added to the snow) did indeed show that in both seasons, 1-butene and *iso*-butene mixing ratios followed a diurnal trend in snow, peaking at around solar noon. However, their background concentrations (on the order of 100 pptv) were small relative to the levels measured at probe 1 and 2 (on the order of 2500 and 1000 pptv, respectively), when the hydrocarbon doping mix was being added (Fig. 3). Even so, background values were subtracted from the hydrocarbon addition concentrations. The standard errors for sinusoidal fits to the measured background concentrations were about 6 pptv in summer and 20 pptv in spring. These errors contributed only 1–2% to the error in $\ln([A]_2/[A]_1)$, which is small compared to the approximately 30% error associated with fitting the slope to a plot of Eq. (3), so they were not used in further error propagation. In both summer and spring, the background levels for

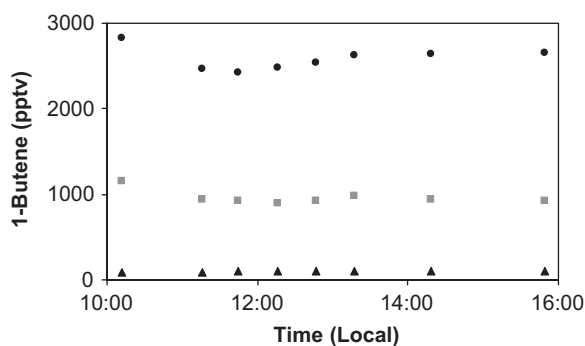


Fig. 3. 1-butene mixing ratios measured at probe 1 (circles) and 2 (boxes) during an experiment performed on 15 April, 2004. Triangles represent the background concentration of 1-butene used to correct for natural production.

Table 1
Kinetic data used for the hydroxyl approximation for the temperature dependency: $k(T) = A \exp^{-B/T}$

	k_{OH} (298 K) 10^{-12} cm^3 $\text{molecule}^{-1} \text{ s}^{-1}$	A 10^{-12} cm^3 $\text{molecule}^{-1} \text{ s}^{-1}$	B (K)
1-butene	31.4	6.55	−467
<i>iso</i> -butene	51.4	9.47	−504
<i>cis</i> -2-butene	56.4	11.0	−487
<i>trans</i> -2-butene	64.0	10.1	−550

cis- and *trans*-2-butene were rarely observed above the 3 pptv limit of detection, therefore no correction was needed.

Plots of $\ln([A]_2/[A]_1)$ versus k_{OH} for the four butenes were used to calculate hydroxyl concentrations in the snow (Eq. (3)). The temperature-dependent kinetic data used are shown in Table 1 (Atkinson, 1997). Temperature measurements from a similar OP4 chamber, employing thermocouple gauges at a number of depths inside the chamber, were used to determine appropriate temperature dependant rate constants. Temperature readings from inside the chamber were used rather than in the undisturbed snow because this allowed for understanding the effect of the chamber's placement on the temperature of the snow. Fig. 4 shows results from an experiment performed on 14 April, 2004. Each line represents the least-squares fit to data from an individual simultaneous probe sampling period. The slope of the line decreases as it gets later in the day because of a decline in OH. The slopes

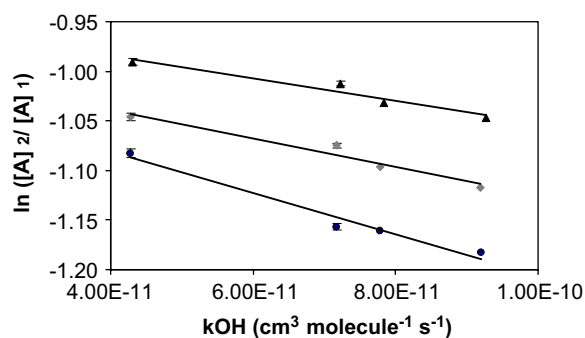


Fig. 4. A plot of the natural log of probe 2 concentration over probe 1 concentration for butenes versus reaction rate with hydroxyl (the butenes are from left to right: 1-butene, *iso*-butene, *cis*-2-butene, and *trans*-2-butene). Circles represent values from 14:16, diamonds 15:17, and triangles 16:20 local time. Error bars show error in hydroxyl values from subtraction of the natural 1-butene and *iso*-butene abundance.

Table 2
Overview of hydroxyl experiments performed at Summit

Date	Duration (local time)	SF6 tests
July 10, 2003	12:00–19:00	Performed on July 9
July 11, 2003	9:00–22:00	Performed on July 9
July 12, 2003	19:00–22:00	Performed on July 9
April 14, 2004	8:00–24:00	Performed on April 13 and 15
April 15, 2004	9:00–16:00	Performed on April 13 and 15
April 27, 2004	5:00–24:00	Performed on April 25 and May 1
April 30–May 1, 2004	0:00 (30th)–1:00 (1st)	Performed on April 25 and May 1
May 1, 2004	12:00–15:00	Performed on April 25 and May 1

were then used to calculate $[OH]$ (Eq. (4)) as it changes diurnally during each experiment.

6. Results

In total, 8 hydrocarbon doping experiments were performed in 2003 and 2004 (see Table 2 for details). Summertime (10–12 July, 2003) OH mixing ratios followed a diurnal cycle, with peak values of 3.2×10^6 molecules cm^{-3} (Fig. 5). This maximum was at 15:00 local time, which was later in the day than typical peak values seen in spring (Figs. 6 and 7). However, it is not certain whether this shows a significant shift in the diurnal hydroxyl peak, because relatively few experiments were performed

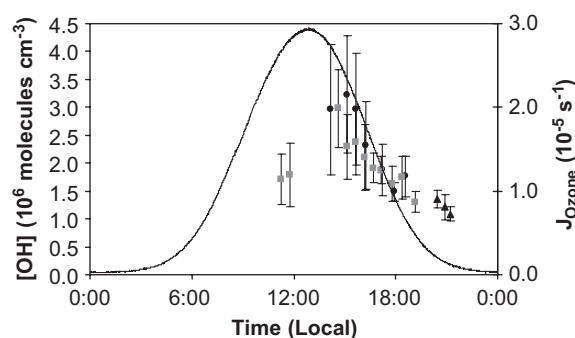


Fig. 5. Hydroxyl values measured on 10 July (circles), 11 July (squares), and 12 July (triangles), 2003. Error bars represent propagated 1σ error in the slope of the line and in residence time. Ozone photolysis rates J_{Ozone} on 10 July are indicated by the line.

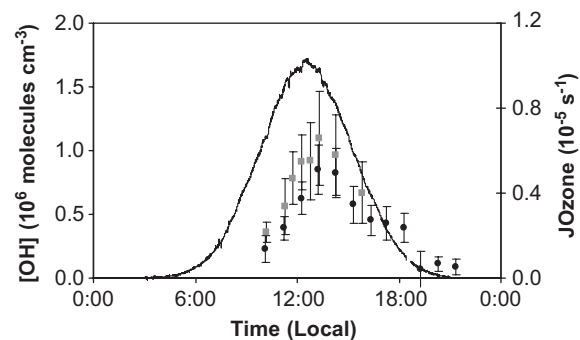


Fig. 6. Hydroxyl values measured on 14 April (circles) and 15 April (squares), 2004. Error bars represent propagated 1σ error in the slope of the line and in residence time. Ozone photolysis rates J_{Ozone} on 14 April are indicated by the line.

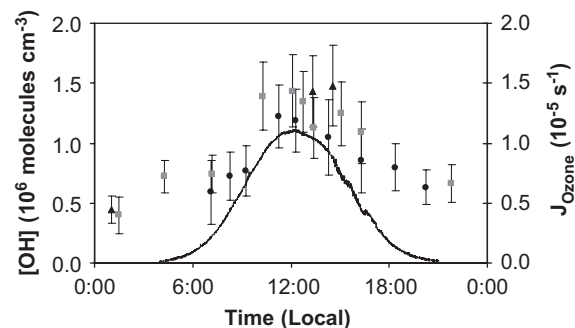


Fig. 7. Hydroxyl values measured on 27 April (circles), 30 April (squares), and 1 May (triangles), 2004. Error bars represent propagated 1σ error in the slope of the line and in residence time. Ozone photolysis rates J_{Ozone} on 27 April are indicated by the line.

between 12:00 and 15:00 in summer. The minimum OH value estimated during summer was 1.1×10^6 molecules cm^{-3} at 20:00 local time. Results during mid-spring (14–15 April, 2004) showed peak hydroxyl mixing ratios of 1.1×10^6 molecules cm^{-3} in the early afternoon (Fig. 6). Late spring (27 April–1 May, 2004) OH peaked at 1.5×10^6 molecules cm^{-3} in the early afternoon (Fig. 7). The error bars in Figs. 5–7 were calculated by propagating the standard deviation in the slope of the line fitting the natural logs to the k_{OHs} and the error in flow chamber residence time.

7. Discussion

Average daily hydroxyl concentrations measured in the snowpack increased during the spring and were highest during summer (Fig. 8). Error bars (Fig. 8) represent the highest and lowest hydroxyl values on each day. Hydroxyl concentrations estimated for the summer experiment were always above 1.0×10^6 molecules cm^{-3} , even at 21:00 local time. This reflects the fact that during the summer, Summit has continuous sunlight and therefore continuous hydroxyl production in the snowpack. By comparison, during the spring the shorter days cause hydroxyl concentrations to decline to very low levels at night. The highest hydroxyl concentrations were reported on 10 July (3.2×10^6 molecules cm^{-3}). However, it is believed that hydroxyl concentrations in the snowpack would be greatest around the summer solstice when the radiative flux is at its greatest. In fact, the highest J values for the photolysis of ozone occurred between 26 June and 5 July, 2003.

Direct ambient hydroxyl measurements made on 30 April, 2004 with a chemical ionization mass spectrometer (CIMS, described in Sjostedt et al., 2007) followed a diurnal trend with peak values at a similar time to those measured on the same day in the firn air (Fig. 9). However, ambient values are significantly higher than the corresponding firn concentration. Average ambient and firn OH values are similar in early spring, while in late spring ambient values are higher by 30–50% (Fig. 10). Summer ambient values increased much faster and were three times as high as firn values on 10 July.

The relatively lower concentrations of OH in the firn air could be the result of a much shorter OH lifetime in the firn air compared to its ambient lifetime. The lifetime of OH due to chemical reaction with trace gases alone in interstitial air and firn air is

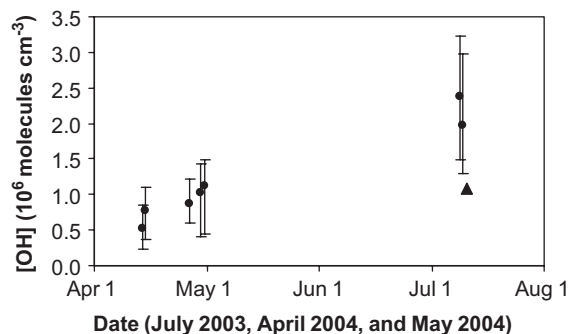


Fig. 8. Average hydroxyl estimates in firn for each day when experiments were performed (circles). Error bars represent the maximum and minimum values seen. On 12 July, 2003 experiments were only performed between 20:00 and 22:00. Therefore only the minimum is shown (triangle). Three values from 14 April were not included because of high error in the individual values.

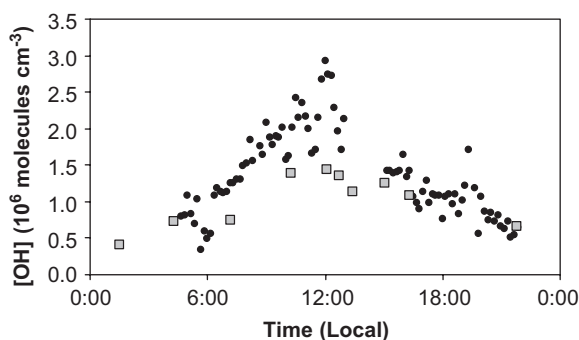


Fig. 9. Ambient hydroxyl measurements made using CIMS (circles) and firn values (boxes) on 30 April, 2004. Between 13:00 and 15:00 local time, pollution was seen from the camp. This caused an increase in ambient OH (not shown).

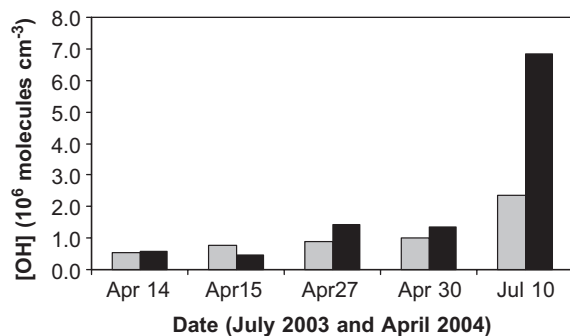


Fig. 10. Daily average hydroxyl values measured in firn (gray bars) and ambient (black bars) air. Averages for ambient OH were for measurements made between 8:00 and 20:00 local time which corresponds to the time when most of the firn hydroxyl experiments were performed.

on the order of 1 s. This is based on values of NMHCs and CO, which were measured in the same stainless-steel canisters as the hydroxyl approximation during periods when the hydrocarbon mix was not being added to the snow. This lifetime also takes into account firn air values of NO measured by a chemiluminescence detector (Ryerson et al., 2000) and ozone measured by a commercially available instrument (Thermo-Environmental Model 49). However, if the hydroxyl in firn air preferentially partitions onto a quasi-liquid layer on the surface of the snowgrains, the firn air OH lifetime could be decreased to a value on the order of 1 ms (C. Anastasio, personal communication, 2005). During the spring, we expect the influence of such a liquid phase to be minimized at the low ambient temperatures. Accordingly, springtime firn air OH mixing ratios are similar to ambient values. By contrast, in summer an increased surface area of this liquid layer may cause fast loss of OH from firn air, resulting in high ambient OH in comparison to firn OH, as observed. In addition, as previously noted, the addition of reactive NMHCs in our doping mix would titrate some of the OH, such that our OH estimates represent a lower limit. This presumably would have a similar influence on both spring and summer experiments, so it does not explain the spring vs. summer ambient vs. firn differences.

This work demonstrates that significant levels of OH are present in the air between surface snow grains. In combination with the high levels of nitrogen oxides (Dibb et al., 2002), radical precursors (HONO and H₂O₂), and photochemical products (alkyl nitrates and HCHO) that have been observed in firn air it supports the conclusion that active photochemistry is occurring just below the snow surface. These processes have been suggested to possibly alter ice core records of chemical indicators such as hydrogen peroxide (Anastasio and Jordan, 2004), meaning that snow and ice can not be assumed to be the inert freezer of past conditions they once were, but rather are a reactive environment whose chemistry is not yet fully understood.

With as much as 50% ($46 \times 10^6 \text{ km}^2$) of the Northern Hemisphere land surface snow-covered (Frei and Robinson, 1999) and approximately $12 \times 10^6 \text{ km}^2$ of sea ice during the winter (Vinnikov et al., 1999), this work also suggests that photochemical activity involving snow surfaces is widespread during late winter and early spring as solar radiation and temperature increases. For locations

such as Summit, hydroxyl precursors originate predominantly from anthropogenic sources, however, snow-covered areas in less remote sites will see reactions involving both anthropogenic and biological products that must be studied in detail. These complex reactions could cause the snow to play a significant role in the chemistry of the boundary layer above it.

8. Conclusions

Experiments performed during two field seasons (spring and summer) at Summit, Greenland employed an indirect technique, adding a mixture of butenes to near-surface firn air, to infer peak hydroxyl levels of $1.5 \times 10^6 \text{ molecules cm}^{-3}$ in April and May and $3.2 \times 10^6 \text{ molecules cm}^{-3}$ in July. Ambient OH levels measured by a direct CIMS method are similar to our firn estimates in spring, but the difference increases in summer, such that ambient hydroxyl is approximately three times as large as our firn hydroxyl mixing ratios. We speculate that enhanced interaction between liquid water on the surface of snowgrains in summer may decrease the summer firn OH lifetime, thus decreasing steady-state levels in this interstitial environment. This work makes an important contribution to current understanding of snowpack photochemical and physiochemical processes.

Acknowledgments

This research was funded by NSF Grant 0220862 through the Office of Polar Programs. None of the research would be possible without excellent logistical support from VECO, the support of the Greenland home rule, and the sweet ride provided by the Air National Guard 109th. Thanks are also due to Mac Cathles, Zoe Courville, and Sarah Story for assistance during both field campaigns and to Mary Albert for temperature measurements and equipment needed for the SF₆ tests. Invaluable analytical support at UC Irvine was provided by Brent Love, Kevin Gervais, Gloria Liu, David Medina, Angela Baker, and Brian Novak.

References

- Anastasio, C., Jordan, A.L., 2004. Photoformation of hydroxyl radical and hydrogen peroxide in aerosol particles from Alert, Nunavut: implications for aerosol and snowpack

- chemistry in the Arctic. *Atmospheric Environment* 38, 1153–1166.
- Atkinson, R., 1997. Gas-phase tropospheric chemistry of volatile organic compounds: 1. alkanes and alkenes. *Journal of Physical and Chemical Reference Data* 26, 215–290.
- Blake, N.J., Swanson, A.L., Blake, D.R., Peterson, M.C., Hosjonrath, R.E., Dibb, J.E., Shepson, P., 1999. Hydroxyl radical concentrations associated with surface snow at summit, Greenland Determined from addition of reactive hydrocarbons. *EOS Transactions of the American Geophysical Union, Fall Meeting, Supplement, vol. 80, Abstract A52D-09*.
- Colman, J.J., Swanson, A.L., Meinardi, S., Sive, B.C., Blake, D.R., Rowland, F.S., 2001. Analysis of a wide range of volatile organic compounds in whole air samples collected during PEM-tropics A and B. *Journal of Analytical Chemistry* 73, 3723–3731.
- Dibb, J.E., Arsenaault, M., Peterson, M.C., Honrath, R.E., 2002. Fast nitrogen oxide photochemistry in Summit, Greenland snow. *Atmospheric Environment* 36, 2501–2511.
- Frei, A., Robinson, D.A., 1999. Northern Hemisphere snow extent: regional variability 1972–1994. *International Journal of Climatology* 19, 1535–1560.
- Hutterli, M.A., Röthlisberger, R., Bales, R.C., 1999. Atmosphere-to-snow-to-firn transfer of HCHO at Summit, Greenland. *Geophysical Research Letters* 26, 1691–1694.
- Hutterli, M.A., McConnell, J.R., Stewart, R.W., Jacobi, H.-W., Bales, R.C., 2001. Impact of temperature-driven cycling of hydrogen peroxide (H₂O₂) between air and snow on the planetary boundary layer. *Journal of Geophysical Research* 106, 15395–15404.
- Jacobi, H.-W., Frey, M.M., Hutterli, M.A., Bales, R.C., Schrems, O., Cullen, N.J., Steffen, K., Koehler, C., 2002. Measurements of hydrogen peroxide and formaldehyde exchange between the atmosphere and surface snow. *Atmospheric Environment* 36, 2619–2628.
- Mauldin III, R.L., Kosciuch, E., Henry, B., Eisele, F.L., Shetter, R., Lefer, B., Chen, G., Davis, D., Huey, G., Tanner, D., 2004. Measurements of OH, HO₂ + RO₂, H₂SO₄, and MSA at the South Pole during ISCAT 2000. *Atmospheric Environment* 38, 5423–5437.
- Peterson, M.C., Honrath, R.E., 2001. Observations of rapid photochemical destruction of ozone in snowpack interstitial air. *Geophysical Research Letters* 28, 511–514.
- Ryerson, T.B., Williams, E.J., Fehsenfeld, F.C., 2000. An efficient photolysis system for fast-response NO₂ measurements. *Journal of Geophysical Research* 105, 26447–26461.
- Sive, B.C., 1998. Dissertation: atmospheric NMHC analytical methods and estimated hydroxyl radical concentrations. University of California, Irvine.
- Sjostedt, S.J., Huey, L.G., Tanner, D.J., Pieschl, J., Chen, G., Dibb, J.E., Lefer, B., Hutterli, M.A., Beyersdorf, A.J., Blake, N.J., Blake, D.R., Sueper, D., Ryerson, T., 2007. Observations of hydroxyl and the sum of peroxy radicals at Summit, Greenland during summer 2003. *Atmospheric Environment*, this issue, doi:10.1016/j.atmosenv.2006.06.065.
- Sumner, A., Shepson, P., 1999. Snowpack production of formaldehyde and its impact on the Arctic troposphere. *Nature* 398, 230–233.
- Swanson, A.L., Blake, N.J., Blake, D.R., Albert, M.R., 2000. Reactivity within unconsolidated snow: evidence for heterogeneous and radical chemistry affecting trace gas concentrations. *EOS Transactions of the American Geophysical Union* 81 (48) Fall Meet. Suppl., Abstract A12D-11.
- Swanson, A.L., Blake, N.J., Blake, D.R., Rowland, F.S., Dibb, J.E., 2002. Photochemically induced production of CH₃Br; CH₃I; C₂H₅I; ethene, and propene within surface snow. *Atmospheric Environment* 36, 2671–2682.
- Swanson, A.L., Blake, N.J., Atlas, E., Flocke, F., Blake, D.R., Rowland, F.S., 2003. Seasonal variations of C₂–C₄ non-methane hydrocarbons and C₁–C₄ alkyl nitrates at the Summit research station in Greenland. *Journal of Geophysical Research* 108, 4065–4073.
- Vinnikov, K.Y., Robock, A., Stouffer, R.J., Walsh, J.E., Parkinson, C.L., Cavalieri, D.J., Mitchell, J.F.B., Garrett, D., Zakharov, V.F., 1999. Global warming and Northern hemisphere sea ice extent. *Science* 286, 1934–1937.
- Yang, J., Honrath, R.E., Peterson, M.C., Dibb, J.E., Sumner, A.-L., Shepson, P.B., Frey, M., Jacobi, H.-W., Swanson, A., Blake, N., 2002. Impact of snowpack photochemistry on HO_x levels at Summit, Greenland. *Atmospheric Environment* 36, 2523–2534.
- Zhou, X., Beine, H.J., Honrath, R.E., Fuentes, J.D., Simpson, W., Shepson, P.B., Bottenheim, J.W., 2001. Snowpack photochemical production of HONO: a major source of OH in the Arctic boundary layer in springtime. *Geophysical Research Letters* 28, 4087–4090.